International Research Journal of Advanced Engineering and Science
ISSN (Online): 2455-9024

Thermal and Thermo Hydraulic Performance of Three Sides Artificially Roughened Solar Air Heaters

Ashwini Kumar[1], B. N. Prasad[2], K. D. P. Singh[3]
[1]Research Scholar, Mechanical Engineering Department, N.I.T, Jamshedpur, India-831014
[2]Professor, Mechanical Engineering Department, N.I.T, Jamshedpur, India-831014
[3]Associate professor, Mechanical Engineering Department, N.I.T, Jamshedpur, India-831014

Abstract— *The experimental results on Stanton number, friction factor and thermal performance of three sides artificially roughened and glass covered solar air heaters with those of smooth and three sides glass covered solar air heaters have been represented. Results show that the values of Stanton number are more in three sides roughened one, leading to an increase of 53% to 57% in thermal performance as compared to three sides glass covered smooth one. However, friction factor increases by 28% to 38%. The effect of roughness and flow parameters (p/e, e/D, Re) on heat transfer, friction factor and thermo hydraulic performance has been shown and discussed. The optimal thermo hydraulic performance of such solar air heaters has been achieved at an optimal value of optimization parameter,* $e^+_{opt} = 23$.

Keywords— *Stanton number, friction factor, thermal performance, roughness reynolds number, thermo hydraulic performance.*

I. INTRODUCTION AND LITERATURE REVIEWS

Use of artificial roughness of different configurations have been used in plenty of studies to enhance the heat transfer rate in solar air heaters during the last decades. Varying magnitudes of roughness results in varying values of heat transfer and friction factor enhancement. An enhancement of about double than that of smooth solar air heater with respect to heat transfer coefficient have been reported [1], [2], while the friction factor quadrupled. Heat transfer and friction factor correlations have been obtained for V-rib roughened solar air heaters [3]. The effect of different orientation of W-rib roughness has been investigated to enhance heat transfer in solar air heaters [4]. Review reports on roughness geometries used in solar air heaters are available [5], [6]. CFD based analysis for heat transfer and friction factor has been made for transverse wire roughness in solar air heaters [7]. Nusselt number and friction factor correlations have been obtained for arc-shaped wire roughness and dimple shaped roughness [8], [9]. Reviews [10], [11] for turbulence promoters and effect of roughness geometries on heat transfer enhancement in solar thermal systems give wide range of data and results on heat transfer and friction factor.

Artificial roughness provided on absorber plates invariably enhances heat transfer associated with increase in friction factor. Increase in heat transfer increases the thermal performance but increase in friction factor affects the thermo hydraulic performance. Thermal and thermo hydraulic performance results of roughened solar air heaters have been reported [12-15]. Effect of the roughness parameters (p/e, e/D) and Reynolds number have been represented and discussed in literature to a large extent to arrive at conclusion that increasing values of e/D for a given value of p/e increases heat transfer and friction factor both.

Despite plenty of works dealing with the effect of artificial roughness on heat transfer and friction factor in solar air heaters, very few dealt with the thermo hydraulic performance in them. Based on the approach adopted [16-18], analysis for the optimal thermo hydraulic performance in one side roughened solar air heater has been reported [19]. The thermo hydraulic optimization parameter, $e^+ = \frac{e}{D}\sqrt{\frac{f}{2}}\,\mathrm{Re}$, known as roughness Reynolds number, has been considered to arrive at the optimal thermo hydraulic performance condition. Covering a wide range of the values of heat transfer surface area, overall heat conductance and flow friction power, Webb and Eckert [18] arrived at the conclusion that the value of the parameter, $e^+ = 20$, gives the optimal thermo hydraulic performance. For circular tube roughened surface with ribs, the value of the optimization parameter, $e^+ = 20$, corresponded to the optimal thermo hydraulic condition[17]. Sheriff and Gumley [16] studied for annulus with wire type roughness and found the optimal condition at $e^+ = 35$ Prasad and Saini [19] obtained the value of roughness Reynolds number, $e^+ = 24$, for optimal thermo hydraulic condition. Karmare and Tikekar [20] has optimized the thermo hydraulic performance of solar air heater integrated with metal rib grift on the absorber plate at an angle of 60^0, as roughness element. Results on thermal and thermo hydraulic performance of wavy finned absorber plate solar air heaters have been reported recently [21].

However, in all the above cases, provision of artificial roughness and glass cover has remained limited to only one side (top side) of the solar air heater duct except those of the recent ones [23], [24] wherein it has been concluded that three sides roughened and glass covered solar air heaters perform even better than those of one side roughened and glass covered solar air heaters, but friction factor also increases. The authors [25] analysis could reveal that, $e^+_{opt} = 23$ corresponds to the optimal thermo hydraulic performance in three sides artificially roughened and glass covered solar air heaters. Table 1 summarizes the value of the parameter, e^+, obtained under varying conditions of roughness and flow parameters corresponding to the optimal thermo hydraulic condition. The value of the parameter, e^+, depends on the combined effect of the roughness and flow parameters.

Ashwini Kumar, B. N. Prasad, and K. D. P. Singh, "Thermal and thermo hydraulic performance of three sides artificially roughened solar air heaters," *International Research Journal of Advanced Engineering and Science*, Volume 2, Issue 2, pp. 215-231, 2017.

International Research Journal of Advanced Engineering and Science
ISSN (Online): 2455-9024

Since, the three sides roughened and glass covered solar air heater is novel one compared to one side roughened solar air heaters, available in literature, its thermohydraulic performance condition is required to be investigated with a view to verify the analysis [25] for optimal thermo hydraulic performance condition at $e^+ = 23$ As such, experiment has been conducted on such solar air heater and the present paper deals with the experimental results obtained with respect to heat transfer, Stanton number, friction factor, thermal performance and finally thermo hydraulic performance to validate that, $e^+ = 23$, corresponds to the optimal thermo hydraulic performance condition in three sides roughened and glass covered solar air heaters.

TABLE 1.Values of e^+_{opt} for different roughness geometries for fully developed turbulent flow.

Sl.No.	References	Roughness and flow duct geometry	p/e	e/D	Re	e^+_{opt}
1.	Sheriff and Gumley[16]	Annulus with wires	10	0.018-0.035	1×10^4–2×10^3	35
2.	Webb and Eckert [18]	Rectangular with ribs	10-40	0.01-0.04	6×10^3–10×10^3	20
3.	Lewis[17]	Circular tubes with ribs	2-60	0.02-0.10	1×10^4–1×10^7	20
4.	Prasad and Saini [19]	Rectangular with top side wires	10-40	0.020-0.033	3×10^3–20×10^3	24
5.	Verma and Prasad [22]	Rectangular with top side wires	10-40	0.010-0.030	5×10^3–20×10^3	24
6.	Prasad et al.[25]	Rectangular with three sides wires	10-40	0.010-0.028	3×10^3–20×10^3	23
7.	Present case	Rectangular with three sides wires	10-30	0.013–0.025	4×10^3–20×10^3	23

II. METHODOLOGY

The experimental set-up consists of two solar air heater ducts both having aspect ratio value of 8 and similar size : (i) smooth with three sides glass covers and (ii) three sides roughened with three sides glass covers as shown in Figs. 1(a) and (b). Fig. 2(a) and (b) show the schematic and photograph of the experimental set- up respectively with measuring instruments and run by a single 5 HP blower simultaneously. Mass flow rate was varied by controlling the blower speed by means of a 3-phase auto variac and measured by means of two separate flange tape orifice-meters having discharge coefficient of 0.61. Multi-tube manometers were used to measure the pressure drop along the duct length. Pressure taps as shown in Fig. 3, connected to multitube manometer by means of PVC tubes measured the pressure drop along the collector duct length. Air and plate temperatures were measured by means of 28 SWG copper-constant on thermocouples fed to digital sensors. Intensity of solar radiation was measured by a digital pyranometer, installed at the experiment site. Thermocouple arrangement for the plate temperature measurement has been shown in Fig. 4. Test data were obtained outdoor on the roof of a building on clear sky days between 11 AM and 2 PM during the months of February to May 2015. A wide range of experimental data for 105 number of test runs for 15 set of roughened absorber plates were collected simultaneously with the smooth one. The roughness and flow parameters were selected so as to yield a wide range of values of the roughness Reynolds number, e^+ On a single day, test data were collected for a given value of mass flow rate. Table 2 shows the range of parameters investigated.

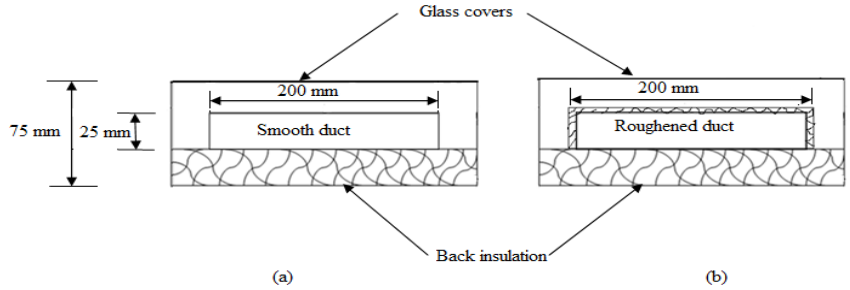

Fig. 1 (a) and (b) Solar air heater duct models.

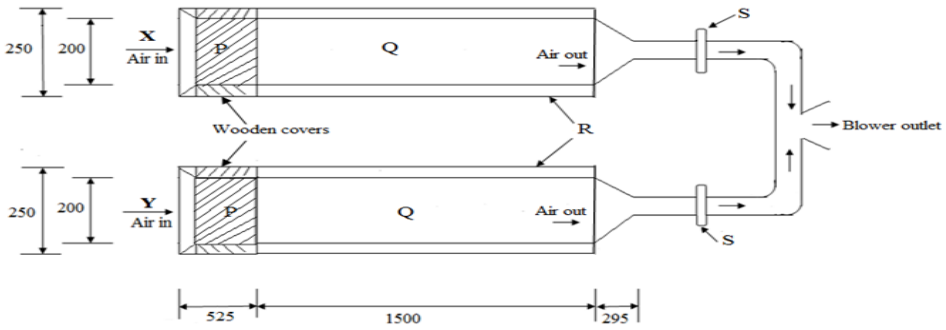

Fig. 2(a). Schematic diagram of the experimental set-up.

All dimensions are in mm

X-Three sides roughened and glass covered solar air heater, **Y**- Smooth and three sides glass covered solar air heater

P- Unheated wooden covered entry section

Ashwini Kumar, B. N. Prasad, and K. D. P. Singh, "Thermal and thermo hydraulic performance of three sides artificially roughened solar air heaters," *International Research Journal of Advanced Engineering and Science*, Volume 2, Issue 2, pp. 215-231, 2017.

Q- Glass covered test section
R- Glass covers
S- Flange tape orifice-meters

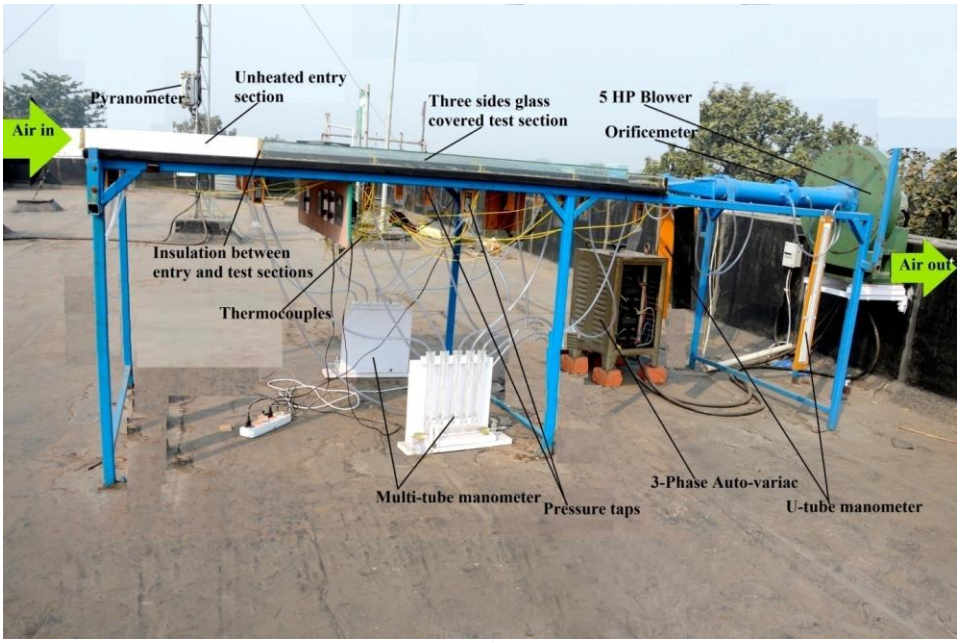

Fig. 2(b). Photograph of experimental set-up.

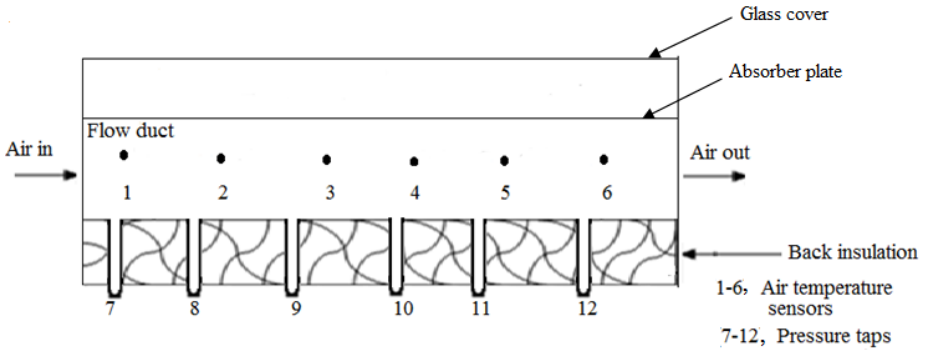

Fig. 3. Arrangement of air temperature sensors and pressure taps along the duct length.

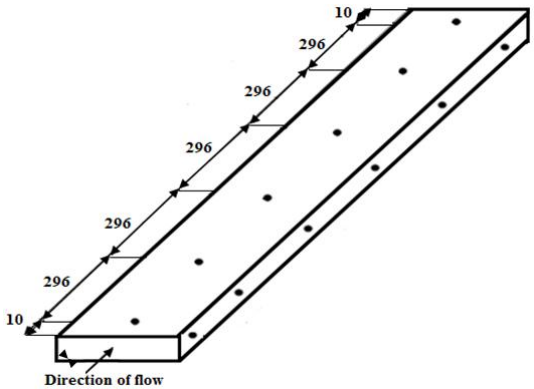

Dimensions are in mm

Fig. 4. Thermocouple arrangement on top and side absorber plate.

TABLE 2. Details of the parameters investigated.

Sl. No	Parameters	Range
1.	Mass flow rate, kg/s	$8.35 \times 10^{-3} - 3.75 \times 10^{-2}$
2.	Reynolds number, Re	4000 – 20000
3.	Roughness height, mm	0.5 – 1.2
4.	Roughness pitch, mm	6 – 30

Ashwini Kumar, B. N. Prasad, and K. D. P. Singh, "Thermal and thermo hydraulic performance of three sides artificially roughened solar air heaters," *International Research Journal of Advanced Engineering and Science*, Volume 2, Issue 2, pp. 215-231, 2017.

5.	Relative roughness pitch, p/e	10 – 30
6.	Relative roughness height, e/D	0.0130 – 0.0250
7.	Roughness Reynolds number, e^+	8.20 – 35.0
8.	Intensity of solar radiation, I, W/m^2	732 – 897
9.	Absorber plate length, L, mm (fixed)	1500
10.	Duct width, W, mm (fixed)	200
11.	Duct height, B, mm (fixed)	25

III. RESULTS

Table 3, showing typically the variation of intensity of solar radiation and ambient temperature is represented by Fig. 5. Fig. 6 shows the instantaneous plate and air temperature in three sides roughened and smooth solar air heaters, across the collector length. Fig. 6 shows that the plate temperature in smooth solar air heater is more than that in three sides roughened one, but air temperature in three sides roughened solar air heater is more than that in smooth one. Higher values of plate temperature and lower values of air temperature in three sides glass covered smooth solar air heater than those in three sides roughened and glass covered solar air heater indicate higher rate of heat transfer in three sides roughened collector than that in smooth collector.

TABLE 3. Typical variation of ambient temperature and intensity of solar radiation during a day.

Time (Hrs.)	11.00	11.15	11.30	11.45	12.00	12.15	12.30	12.45	13.00	13.15	13.30	13.45	14.00
I, W/m^2	786	790	795	801	811	844	877	899	759	742	720	699	648
T_a, ^{0}C	32.9	32.9	33.4	34.1	33.4	33.8	34.1	34.4	34.5	34.6	34.7	34.8	36.1

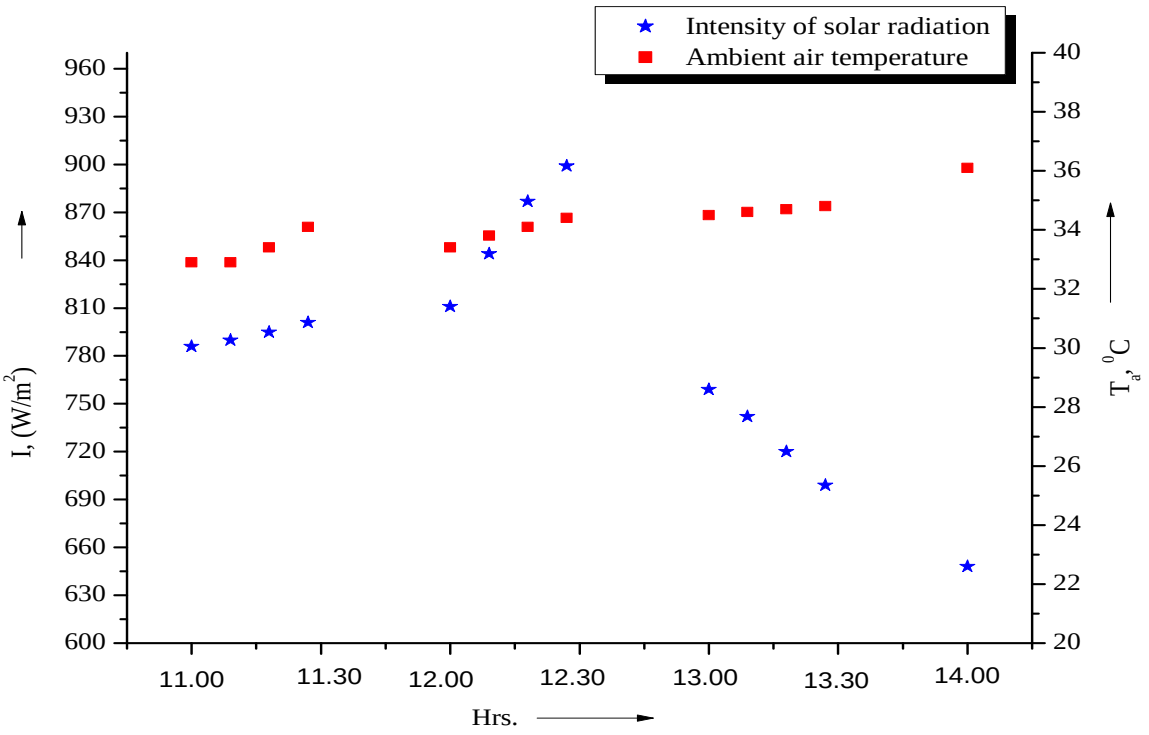

Fig. 5. Typical variation of solar radiation and ambient temperature on a day.

The experimental data with respect to the relative roughness height, relative roughness pitch, flow Reynolds number, intensity of solar radiation, plate and air temperatures, pressure drops along the duct length and orifice-meter have been reduced to obtain the results, using the relevant expressions. The experimental values of heat transfer coefficient have been obtained using the following Eq.(1):

$$\dot{m} C_P \left(T_0 - T_i\right) = h A_C \left(\bar{T}_P - \bar{T}_f\right) \quad (1)$$

where, the values of mass flow rate, $\dot{m}$, have been worked out by using Eq.(2), written under:

Ashwini Kumar, B. N. Prasad, and K. D. P. Singh, "Thermal and thermo hydraulic performance of three sides artificially roughened solar air heaters," *International Research Journal of Advanced Engineering and Science*, Volume 2, Issue 2, pp. 215-231, 2017.

$$\dot{m} = C_d A_2 \left[\frac{2\rho(\Delta P)}{1-\beta_1^4} \right]^{1/2} \quad (2)$$

where, ΔP is the pressure drop in the orificemeter.

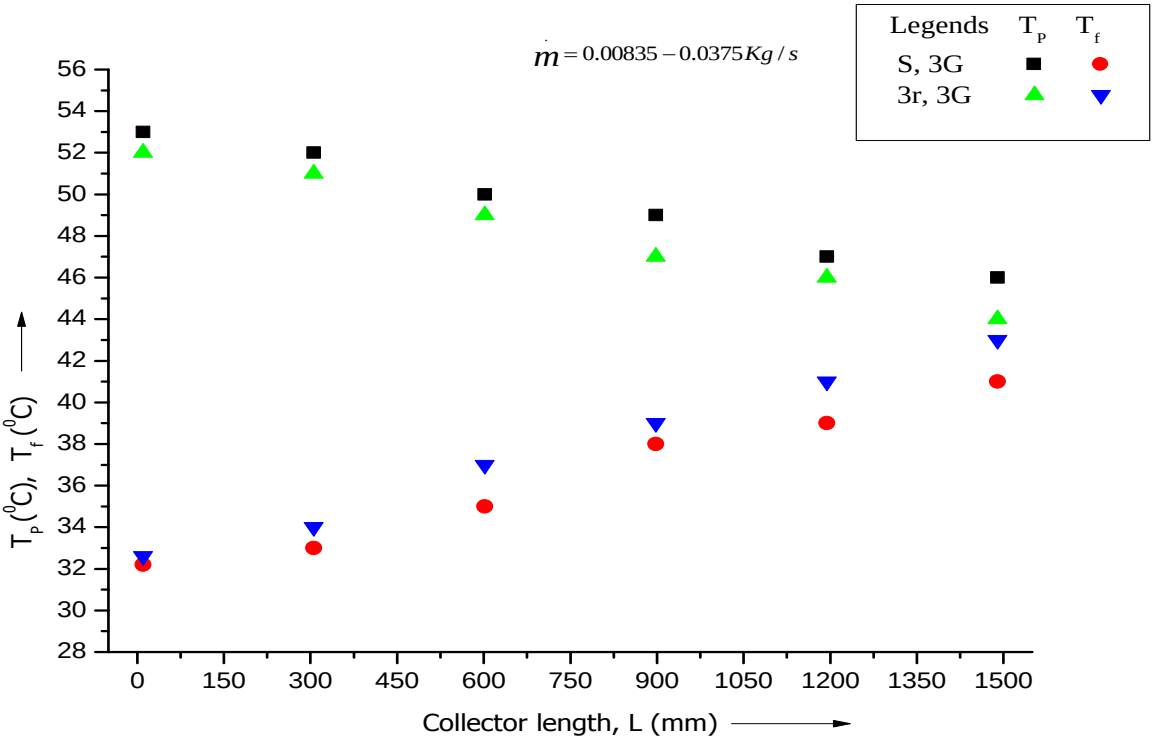

Fig. 6. Instantaneous air and plate temperature in solar air heaters.

The values of heat transfer coefficient, h, have been further used to calculate the values of Nusselt number by the following Eq.(3):

$$Nu = \frac{hD}{K} \quad (3)$$

The values of Nusselt number have been further used to obtain the values of Stanton number by Eq.(4) written under:

$$S_t = \frac{Nu}{Re\, P_r} \quad (4)$$

The respective values of Stanton numbers $\bar{S}_{t_r}$ and S_{t_s}, for the respective solar air heaters have been worked out by Eq.(4). However, to obtain the analytical values of Stanton number, the following Eq.(5) of Prasad et al. [23] has been utilized:

$$\overline{Nu}_r = \left\{ \frac{\bar{fr}/2}{1+\sqrt{\left(\frac{\bar{fr}}{2}\right)}[4.5(e^+)^{0.28} Pr^{0.57} - 0.95\left(\frac{p}{e}\right)^{0.53}]} \right\} Re\, P_r \quad (5)$$

where, $\bar{fr}$, is given by Eq.(6) of Prasad et al. [23], written under:

Ashwini Kumar, B. N. Prasad, and K. D. P. Singh, "Thermal and thermo hydraulic performance of three sides artificially roughened solar air heaters," *International Research Journal of Advanced Engineering and Science*, Volume 2, Issue 2, pp. 215-231, 2017.

International Research Journal of Advanced Engineering and Science
ISSN (Online): 2455-9024

$$\overline{fr} = \frac{(W+2B)\left[\frac{2}{\left\{0.95\left(\frac{p}{e}\right)^{0.53}+2.5\ln\left(\frac{D}{2e}\right)-3.75\right\}^{2}}\right]+Wf_s}{2(W+B)} \quad (6)$$

For smooth solar air heater, the following Eq.(7) [19,25] has been used to obtain the value of S_{t_s} :

$$S_{t_s} = 0.023Re^{0.2}P_r^{-2/3} \quad (7)$$

The experimental values of friction factor, $\overline{fr}$, have been worked out by the following Eq. (8), written under:

$$\Delta P = \frac{4\rho f L V^2}{2gD} \quad (8)$$

where, ΔP is the pressure drop between the inlet and outlet of the collector length and the values of f_s have been obtained by using Eq.(9) of Blasius, as under:

$$f_S = 0.079Re^{-0.25} \quad (9)$$

Figs. 7, 8 and 9 show the comparision of the values of Nusselt number for given values of e/D equal to 0.0225 and p/e equal to 10, 20 and 30 respectively with those of Behura et al. [24]. The experimental values of Nusselt number are seen to compare well in the range of parameters with those of [24]. Figs. 7, 8 and 9 also show the values of Nusselt number for three sides glass covered smooth solar air heater. Similarly, Figs. 10 and 11 show the comparison of friction factor for varying values of p/e equal to 10 and 20 respectively at a given value of e/D equal to 0.0225, which compare well. It needs to mention that, heat transfer and friction factor data of Behura et al. [24] are available for the values of Reynolds number limited to about 12000 only, and both of the heat transfer and friction factor data upto Re = 12000, are very close to each, validating the present data of three sides roughened and glass covered solar air heater for the entire range of Re = 20000. Since, none of any data is available for three sides glass covered smooth solar air heater for direct comparision and the present data for three sides roughened and glass covered solar air heater compare with those of Behura et al. [24], it could very well be assumed that the present data on three sides glass covered smooth solar air heaters (collected simultaneously) would be valid to yield results for such collectors.

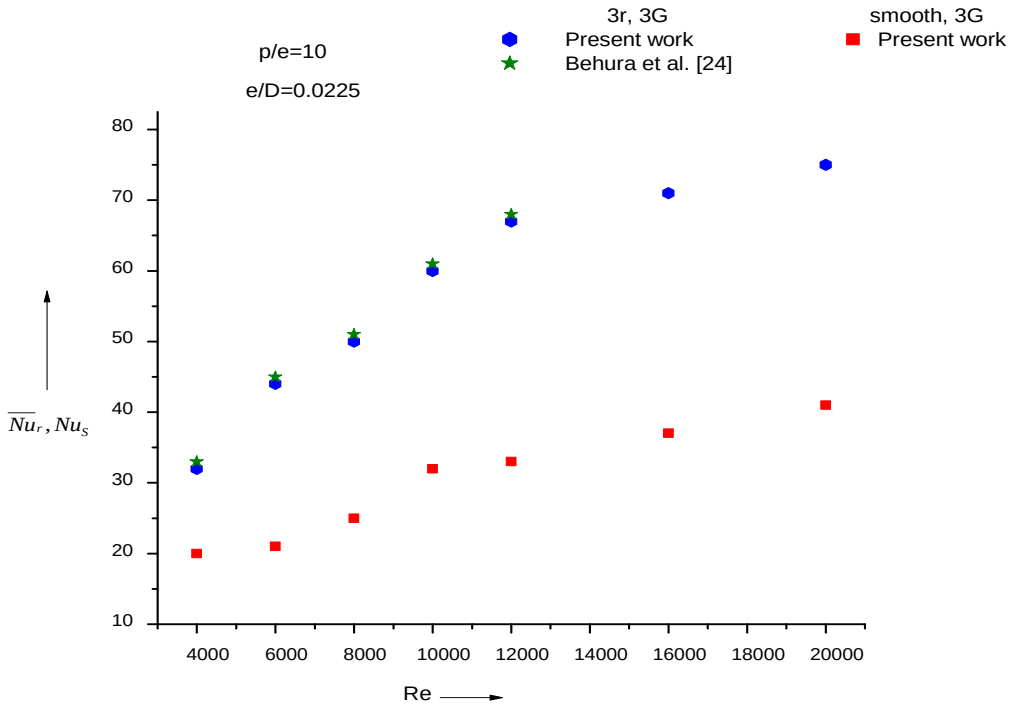

Fig. 7. Comparison of heat transfer data.

Ashwini Kumar, B. N. Prasad, and K. D. P. Singh, "Thermal and thermo hydraulic performance of three sides artificially roughened solar air heaters," *International Research Journal of Advanced Engineering and Science*, Volume 2, Issue 2, pp. 215-231, 2017.

International Research Journal of Advanced Engineering and Science
ISSN (Online): 2455-9024

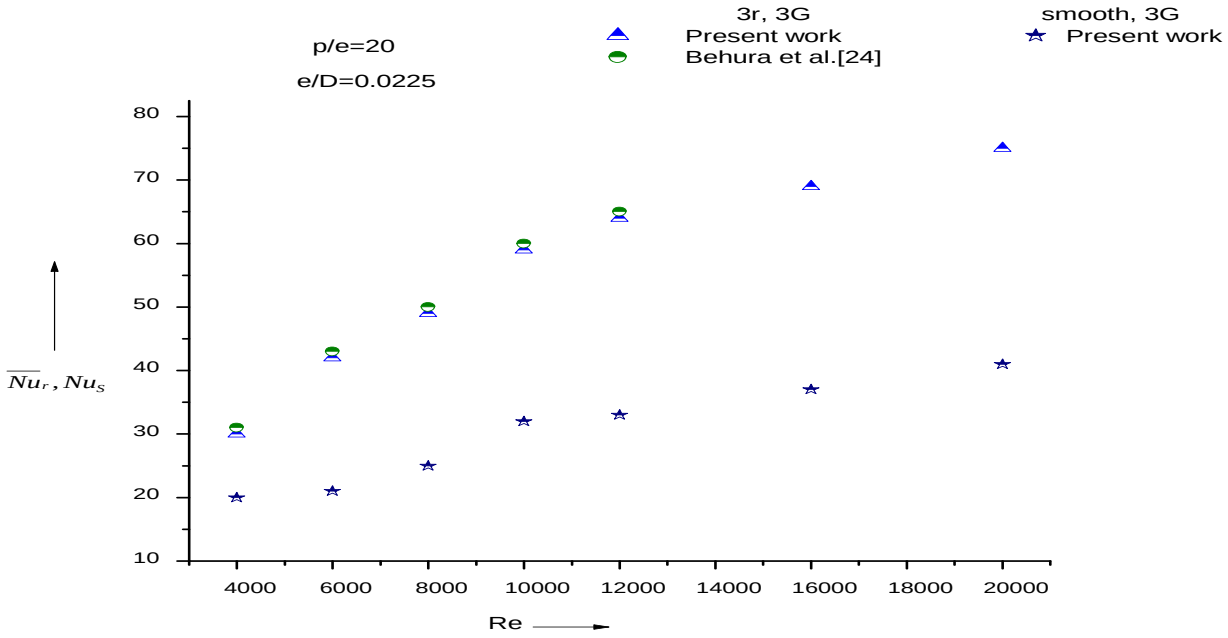

Fig. 8. Comparison of heat transfer data.

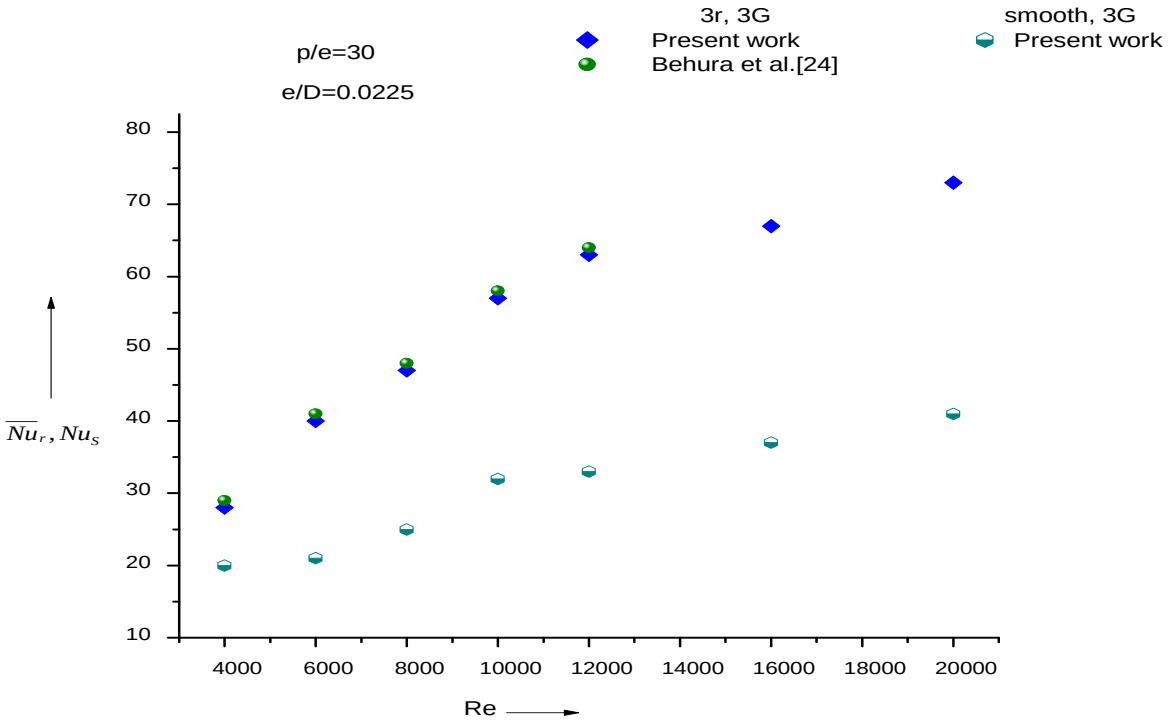

Fig. 9. Comparison of heat transfer data.

Ashwini Kumar, B. N. Prasad, and K. D. P. Singh, "Thermal and thermo hydraulic performance of three sides artificially roughened solar air heaters," *International Research Journal of Advanced Engineering and Science*, Volume 2, Issue 2, pp. 215-231, 2017.

International Research Journal of Advanced Engineering and Science
ISSN (Online): 2455-9024

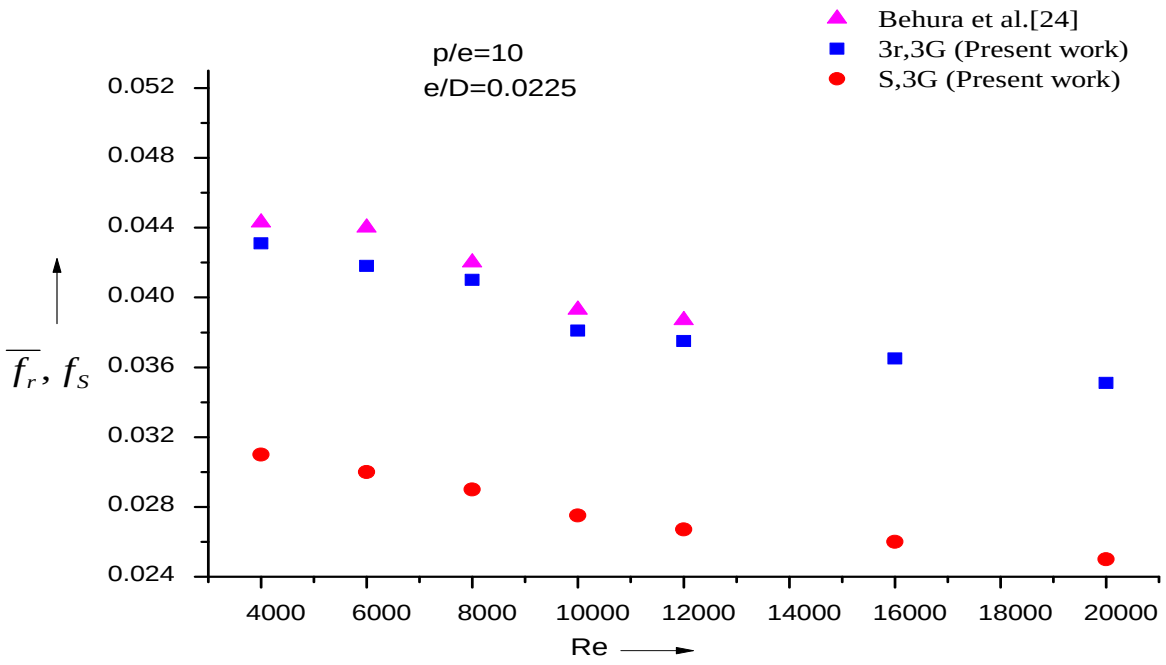

Fig. 10. Comparison of friction factor data.

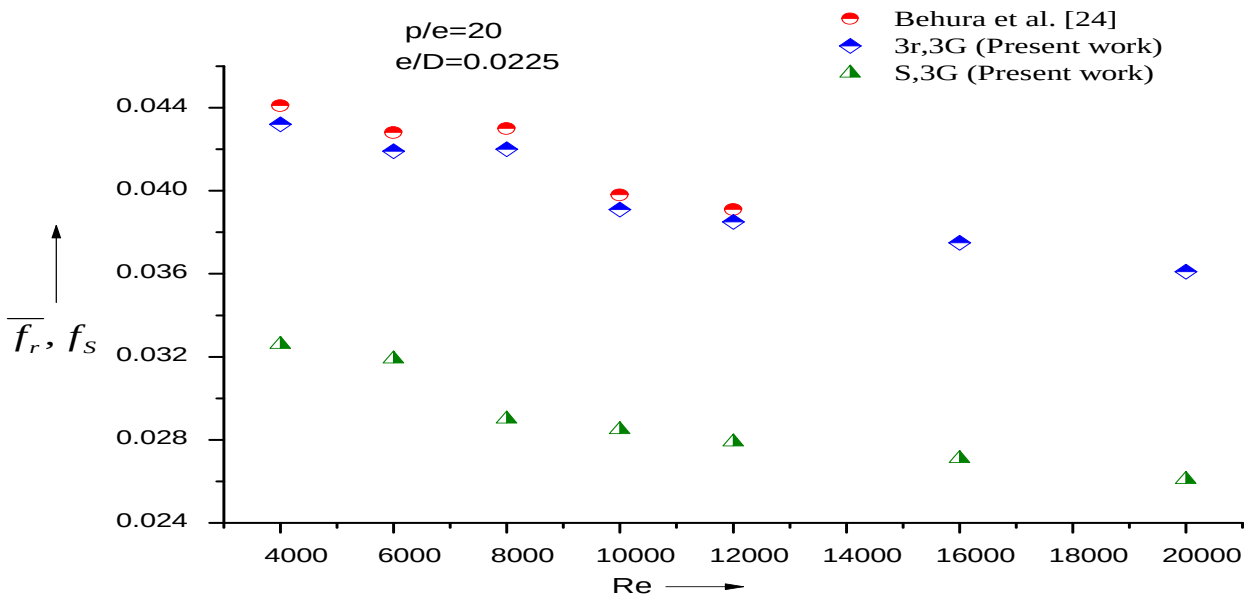

Fig. 11. Comparison of friction factor data.

IV. Discussions on Results

Since, the thermo hydraulic performance of roughened solar air heaters is given by the following Eq.(10),

Ashwini Kumar, B. N. Prasad, and K. D. P. Singh, "Thermal and thermo hydraulic performance of three sides artificially roughened solar air heaters," *International Research Journal of Advanced Engineering and Science*, Volume 2, Issue 2, pp. 215-231, 2017.

$$\eta_{thermo} = \frac{\left(\bar{S}t_r / St_s\right)^3}{\left(\bar{f}r / f_S\right)} \quad (10)$$

results have been shown to see the effect of roughness and flow parameters on Stanton number, friction factor, thermal and thermo hydraulic performance.

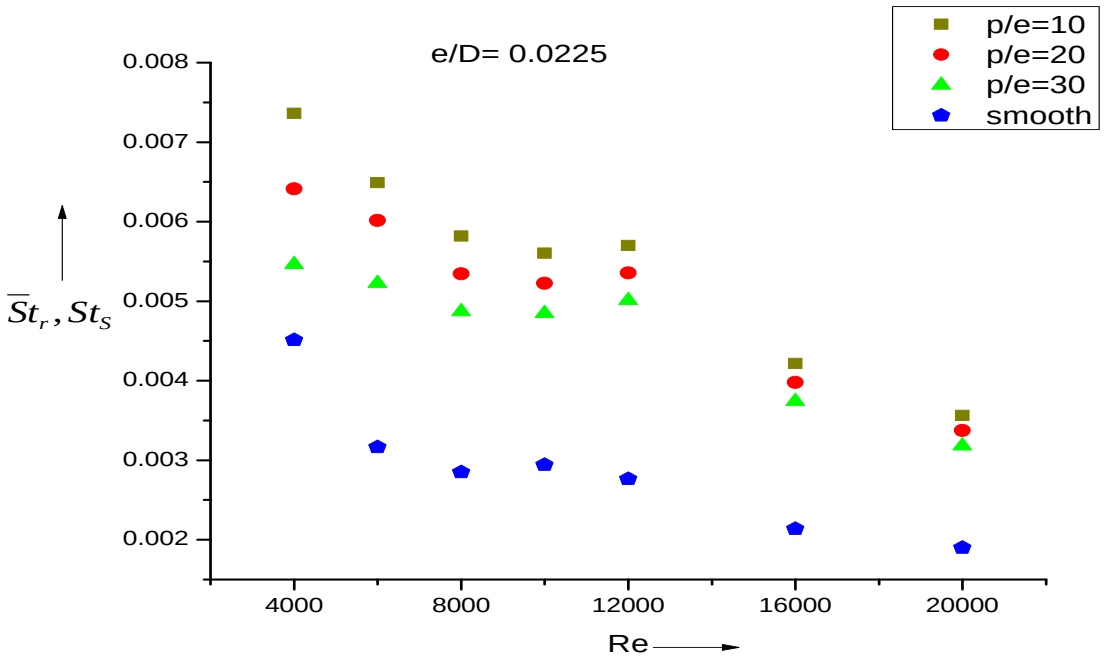

Fig. 12. Effect of p/e on Stanton number in three sides artificially roughened solar air heater.

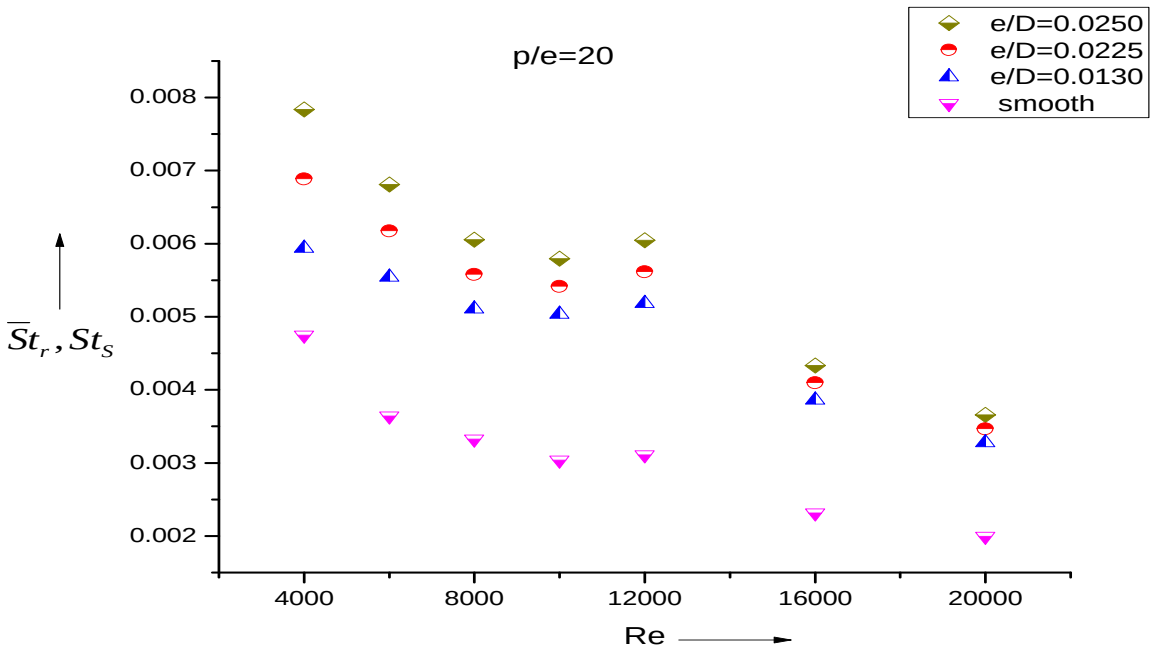

Fig. 13. Effect of e/D on Stanton number in three sides artificially roughened solar air heater.

Ashwini Kumar, B. N. Prasad, and K. D. P. Singh, "Thermal and thermo hydraulic performance of three sides artificially roughened solar air heaters," *International Research Journal of Advanced Engineering and Science*, Volume 2, Issue 2, pp. 215-231, 2017.

International Research Journal of Advanced Engineering and Science
ISSN (Online): 2455-9024

Figs. 12 and 13 show the effect of the roughness and flow parameters p/e, e/D and Re on Stanton number in three sides roughened and smooth collectors. It could be seen from these figures that the values of Stanton number in three sides roughened collector decrease with increasing values of relative roughness pitch, p/e, for a given value of relative roughness height, e/D and decreasing values of relative roughness height, e/D, for a given value of relative roughness pitch, p/e. The values of Stanton number are found to decrease with increasing values of flow Reynolds number. It could be worked out from Figs. 12 and 13, that the values of Stanton number are more in three sides roughened collector in the range of 36% to 65%, as compared to the smooth ones.

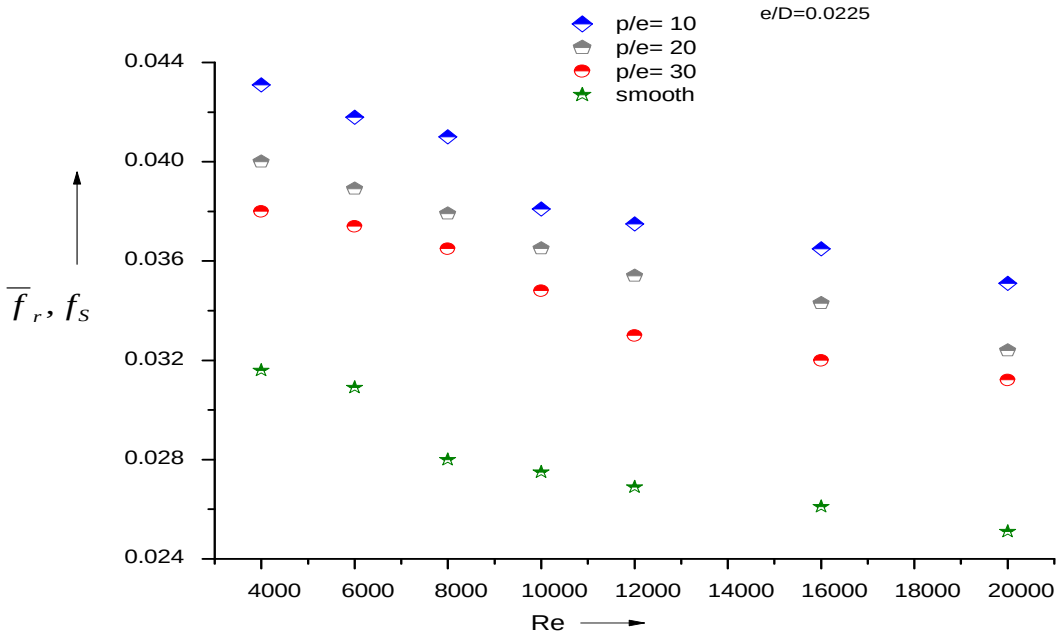

Fig. 14. Effect of p/e on friction factor in three sides artificially roughened solar air heater.

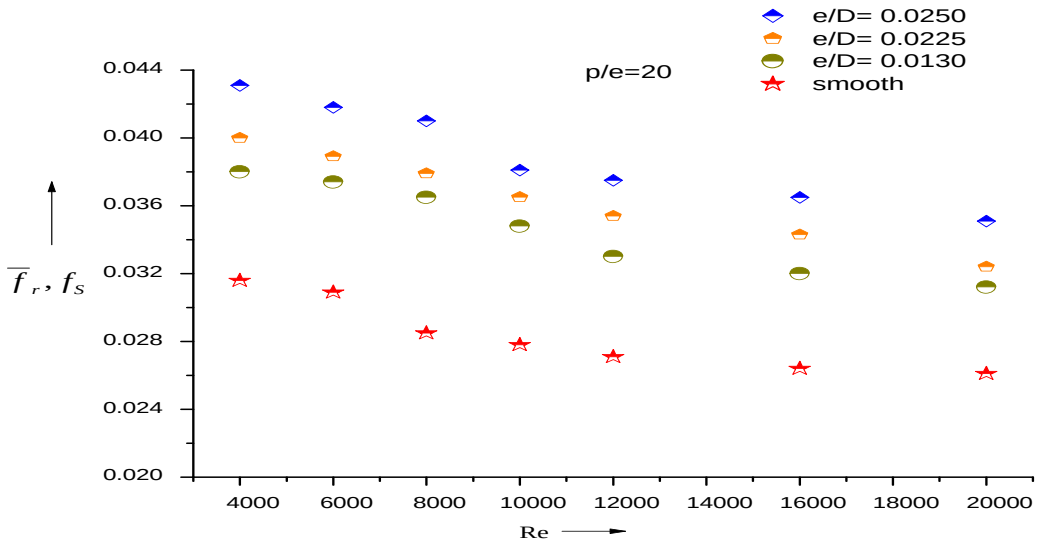

Fig. 15. Effect of e/D on friction factor in three sides artificially roughened solar air heater.

Fig. 14 shows the effect of p/e on friction factor for a given value of e/D, equal to 0.0225. It could be seen from the figure that the values of friction factor increase with decrease in the value of the relative roughness pitch, p/e, and decrease with

Ashwini Kumar, B. N. Prasad, and K. D. P. Singh, "Thermal and thermo hydraulic performance of three sides artificially roughened solar air heaters," *International Research Journal of Advanced Engineering and Science*, Volume 2, Issue 2, pp. 215-231, 2017.

increasing values of the flow Reynolds number, Re. Fig. 15 shows the effect of e/D on friction factor for a given value of p/e, equal to 20. It is quite clear from the figure that the values of friction factor increase with the increase in the value of relative roughness height, e/D and decrease with increasing values of flow Reynolds number, Re. The values of friction factor in three sides roughened collector have been found to increase in the range of 28% to 38%, as compared to the smooth ones.

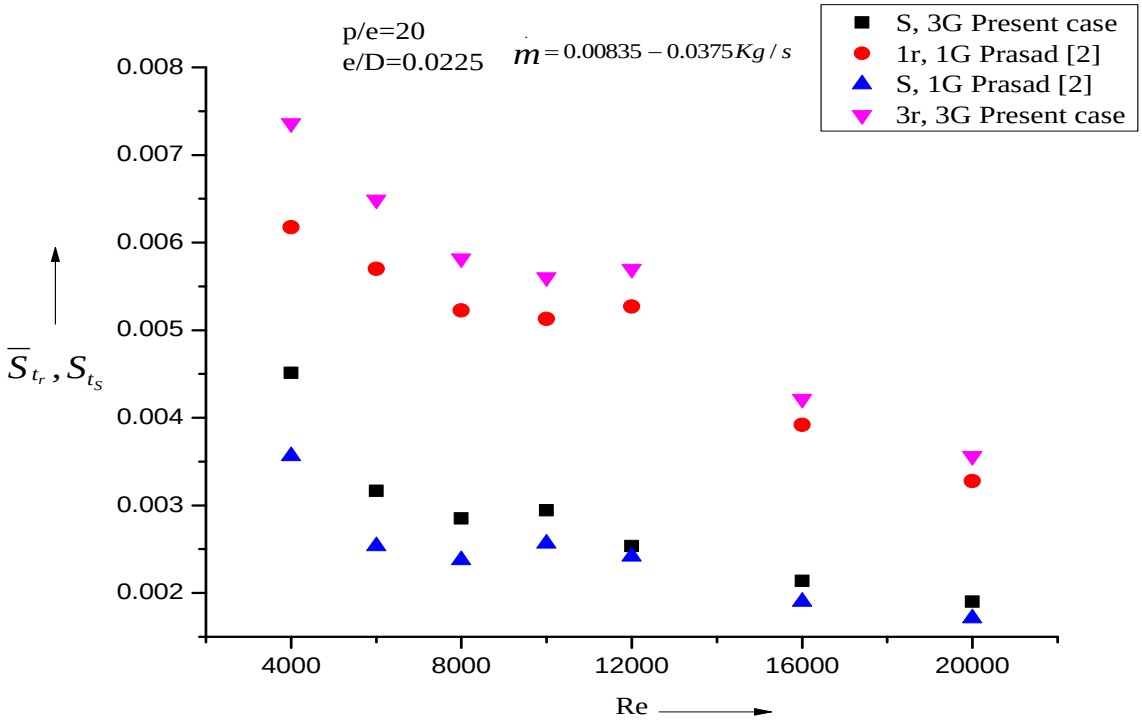

Fig. 16. Effect of roughened sides and glass covers on Stanton number in solar air heaters.

A. Thermal Performance

Three sides artificially roughened and glass covered solar air heaters have been found more efficient than those of only top side roughened ones [23], [24]. This is due to the fact that three sides roughened and glass covered solar air heaters have more absorber plate area and enhanced heat transfer coefficient than those of only one side roughened and glass covered solar air heaters.

The absorber plate area of only top side glass covered roughened as well as smooth[2] solar air heater is equal to:

$$A_C = WL \tag{11}$$

whereas, the absorber plate area of three sides roughened and glass covered solar air heater and the three sides glass covered smooth one is equal to:

$$A_C = WL + 2(BL) \tag{12}$$

The absorber plate area for three sides roughened and glass covered solar air heater and three sides glass covered smooth solar air heater is more by a magnitude of, $2(BL)$, than those of one side glass covered roughened as well as smooth solar air heater, which results in more heat collection for the same value of mass flow rate. Fig. 16 shows the comparative values of Stanton number for the respective solar air heaters. It could be observed from this figure that the solar air heater having three roughened sides and glass covers has the higher value of Stanton number, followed by the solar air heaters: one roughened side and glass cover; smooth and three sides glass covers; smooth and one side glass cover respectively.

Fig. 17 represents typically the performance characteristics of the roughened solar air heaters for p/e =10, e/D = 0.0247: (i) three sides roughened and glass covered, (ii) top side roughened and glass covered, as well as of the smooth solar air heater: (i) smooth and three sides glass covered and (ii) smooth and only top side glass cover, all at varying mass flow rates.

The efficiency data values worked out by the following instantaneous thermal performance Eq. (13):

$$\eta_{th} = \dot{m} C_p (T_0 - T_i) / IA_C \tag{13}$$

shown by the respective lines are represented for each mass flow rate from the origin, resulting in the respective lines for the respective mass flow rates. Utilizing the efficiency data values, the respective curves $A-B_{3r,3G}$, $C-D_{1r,1G}$, $E-F_{S,3G}$ and

Ashwini Kumar, B. N. Prasad, and K. D. P. Singh, "Thermal and thermo hydraulic performance of three sides artificially roughened solar air heaters," *International Research Journal of Advanced Engineering and Science*, Volume 2, Issue 2, pp. 215-231, 2017.

$G-H_{S,1G}$, have been obtained by the least square fit method for three sides roughened and glass covered solar air heater (present case), one side roughened and glass covered solar air heater[2], smooth and three sides glass covered solar air heater (present case) and smooth and only top side glass covered solar air heater[2], respectively. As could be seen from this figure that three sides roughened and glass covered solar air heater has higher value of thermal efficiency than those of only one side roughened and glass covered solar air heater, followed by smooth and three sides glass covered solar air heater having slightly more thermal efficiency than that of smooth and only top side glass covered solar air heater.

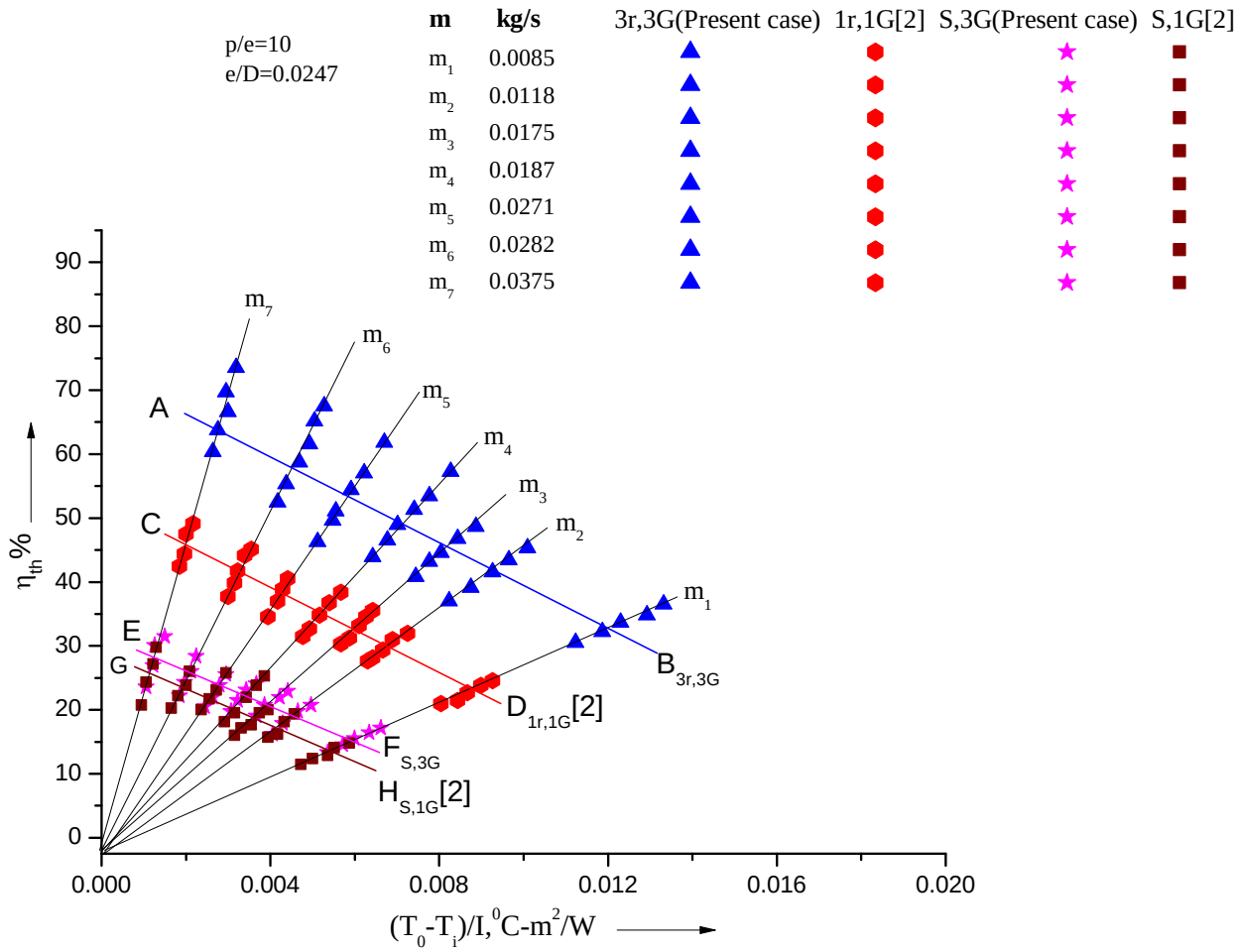

Fig. 17. Performance characteristics of solar air heaters.

Table 4 represents the comparative view of the values of the slope, intercept, collector heat removal factor and collector efficiency factor obtained presently and those of Prasad [2] respectively. Higher values of the parameters, F_R and F', indicate higher value of thermal efficiency.

TABLE 4. Values of slope, intercept, collector heat removal factor and collector efficiency factor.

	Slope, F_0U_L (w/m^{2}K)	Intercept, $F_0(\tau\alpha)$	Collector heat removal factor, F_R	Collector efficiency factor, F'
$3r,3G$ (Present case)	8.56	0.725	0.822	0.918
$1r,1G$ [2]	6.50	0.536	0.545	0.591
$S,3G$ (Present case)	3.94	0.321	0.410	0.504
$S,1G$ [2]	3.60	0.291	0.391	0.496

The values of the thermal performance parameters, F_R and F', given in Table 4 have been worked out by utilizing the following Eqs. (14- 16), [26] written under:

$$F_R(\tau\alpha) = F_0(\tau\alpha)\left[\frac{\dot{m}C_P/A_C}{\dot{m}C_P/A_C + F_0U_L}\right] \quad (14)$$

$$F_RU_L = F_0U_L\left[\frac{\dot{m}C_P/A_C}{\dot{m}C_P/A_C + F_0U_L}\right] \quad (15)$$

$$F' = GC_p\left[\ln\left(\frac{F_0U_L}{F_RU_L}\right)/U_L\right] \quad (16)$$

which further may be used to give the values of $F_R(\tau\alpha)$ and F_RU_L to yeild in the conventional thermal performance Eqs. (17) and (18), for the respective collectors written under:

$$\eta_{th(3r,3G)} = 0.822(\tau\alpha) - \left[0.822U_L\left(\frac{T_i - T_a}{I}\right)\right] \quad (17)$$

$$\eta_{th(S,3G)} = 0.41(\tau\alpha) - \left[0.41U_L\left(\frac{T_i - T_a}{I}\right)\right] \quad (18)$$

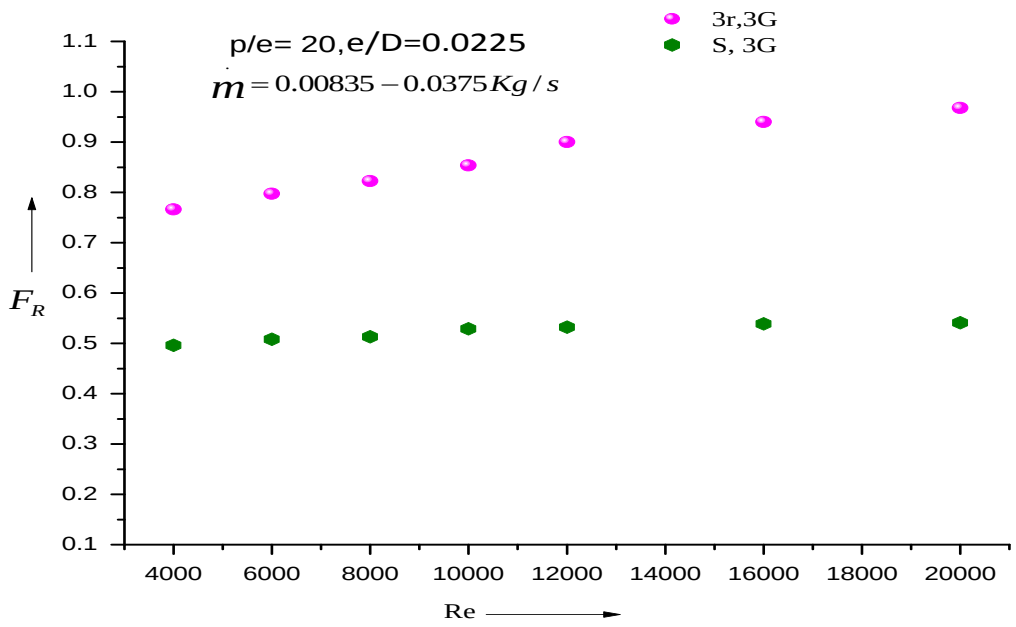

Fig. 18. Collector heat removal factor in solar air heaters.

Figs. 18 and 19 show the values of collector heat removal factor, (F_R) and collector efficiency factor, (F'), respectively for three sides roughened and glass covered solar air heater as well as three sides glass covered smooth solar air heater, as a function of flow Reynolds number. It could be seen that the values of collector heat removal factor, F_R, and collector efficiency factor, F', in three sides roughened and glass covered solar air heater is more as compared to those of the three sides glass covered smooth solar air heater.

The values of the collector heat removal factor, F_R and plate efficiency factor, F', in three sides roughened and glass covered solar air heaters have been found to be more by 51 to 60% and 41 to 49% respectively, as compared to three sides glass covered smooth solar air heater, within the range of the parameters investigated. It could also be attributed that the three sides roughened and glass covered solar air heater is 50 to 59% more efficient than that of the three sides glass covered smooth one.

Ashwini Kumar, B. N. Prasad, and K. D. P. Singh, "Thermal and thermo hydraulic performance of three sides artificially roughened solar air heaters," *International Research Journal of Advanced Engineering and Science*, Volume 2, Issue 2, pp. 215-231, 2017.

International Research Journal of Advanced Engineering and Science
ISSN (Online): 2455-9024

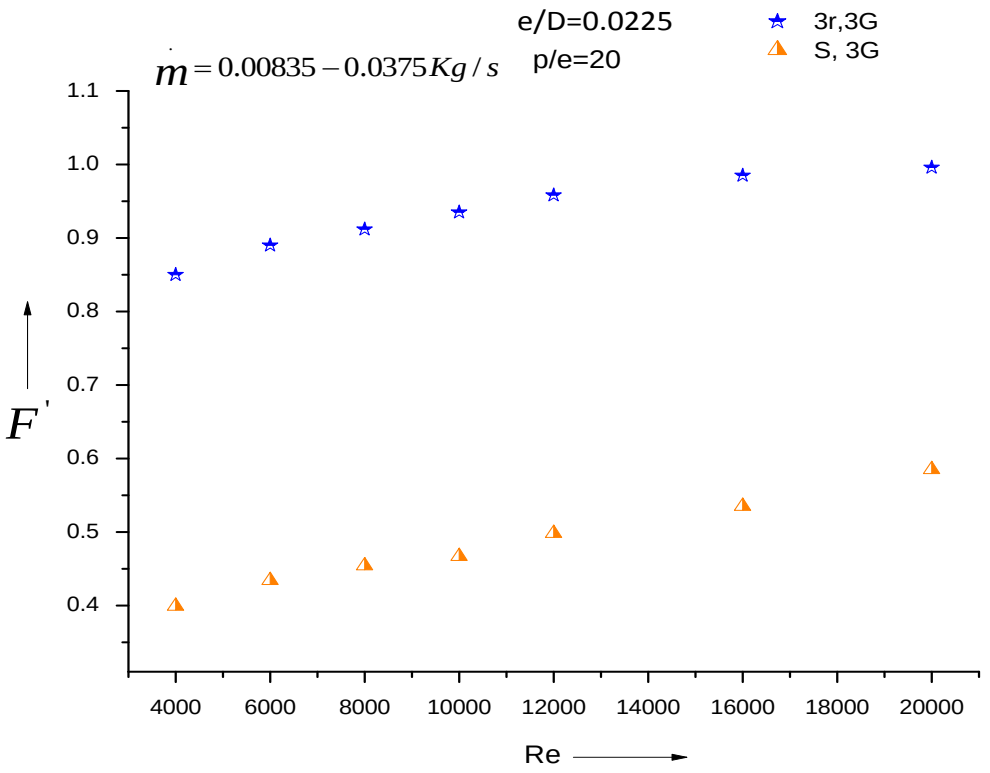

Fig. 19. Collector efficiency factor in solar air heaters.

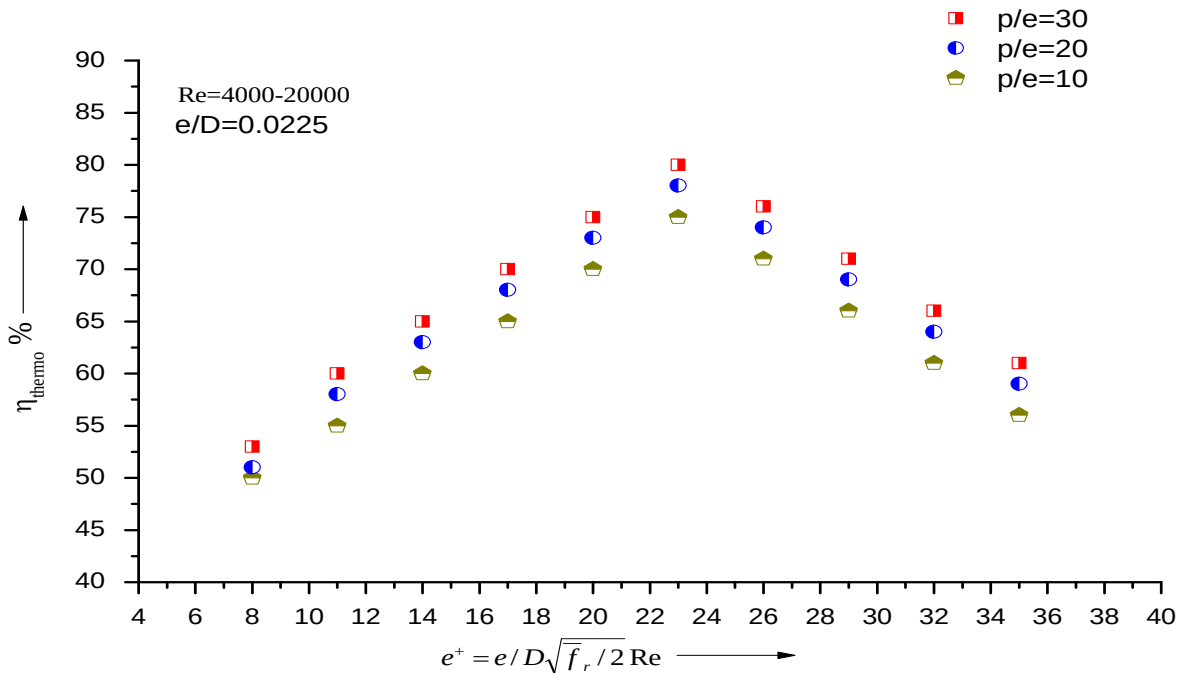

Fig. 20. Effect of p/e and e^+ on thermo hydraulic performance.

Ashwini Kumar, B. N. Prasad, and K. D. P. Singh, "Thermal and thermo hydraulic performance of three sides artificially roughened solar air heaters," *International Research Journal of Advanced Engineering and Science*, Volume 2, Issue 2, pp. 215-231, 2017.

B. Thermo Hydraulic Performance

The values of thermo hydraulic performance worked out by utilizing Eq.(10) have been represented in Figs. 20 and 21, as a function of the parameter, e^+, given by Eq.(19) to see the effect of the parameter, e^+, on thermo hydraulic performance for varying values of p/e and e/D.

$$e^+ = \frac{e}{D}\sqrt{\frac{\bar{f}_r}{2}}Re \tag{19}$$

From Figs. 20 and 21, it could be seen that the value of thermo hydraulic performance increases with increasing values of p/e and e^+, but decreases with increasing values of e/D. It could also be seen from these figures that for every value of p/e and e/D, the value of thermo hydraulic performance increases with increasing values of e^+, and attains the maximum value at $e^+ = 23$, when after, its value decreases for increasing values of e^+. Since, e^+, has remained the optimization parameter to arrive at the optimal thermo hydraulic performance condition in literature, the value of $e^+_{opt} = 23$, could be the optimal value of e^+, to have the optimal thermo hydraulic performance in three sides roughened and glass covered solar air heaters presently.

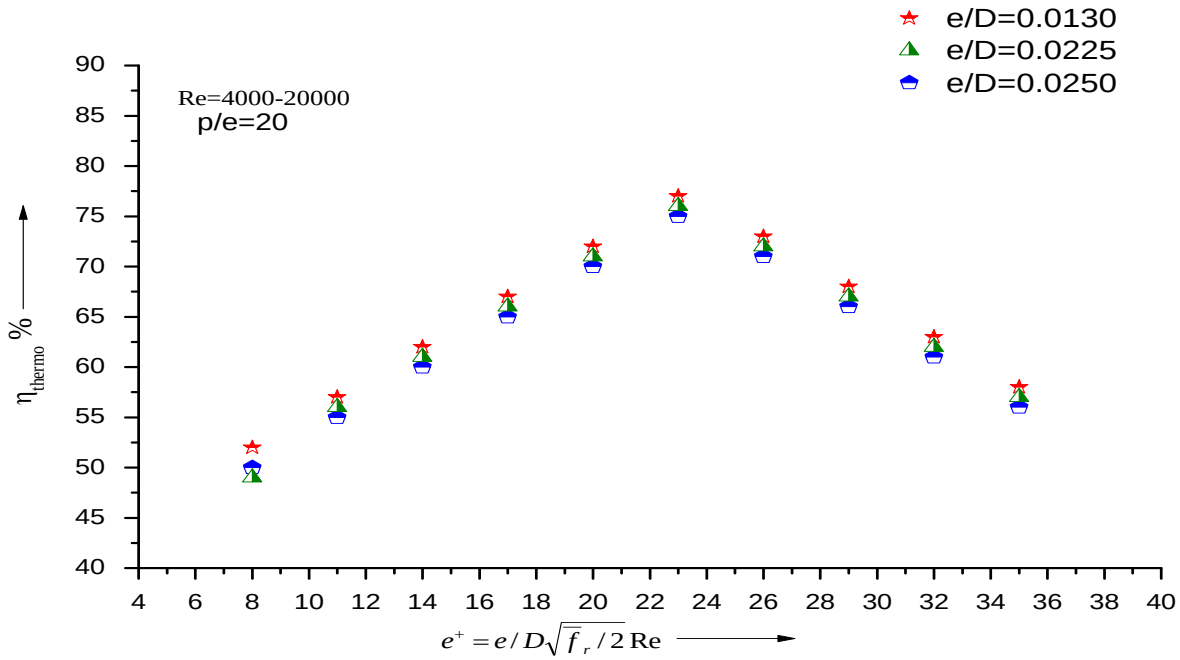

Fig. 21. Effect of e/D and e^+ on thermo hydraulic performance.

Covering the total range of experimental data, Fig. 22 has been drawn to see the effect of the optimization parameter, e^+, on thermo hydraulic performance. It could be seen from this figure that the optimal value of thermo hydraulic performance is achieved at the optimal value of $e^+_{opt} = 23$, which validates the authors[25] analysis. The present optimal value of thermo hydraulic performance in such solar air heaters could be read from this figure to be about 78.8% for optimal value of $e^+_{opt} = 23$.

The value of the optimization parameter, e^+, combines in itself the values of the roughness and flow parameters, under varying conditions of the roughness and flow parameters. As also, the effect of either of the parameters on it may affect the values of other parameters to result in the same value of it. An increase in the value of one parameter, might be compensated by an equivalent decrease in the values of other parameters, to result in the similar value of e^+_{opt}. Since, performance of solar air heaters is very much mass flow rate dependent, flow Reynolds number greatly affects the heat transfer coefficient as well as the friction factor. Results show that heat transfer coefficient increases with increasing values of flow Reynolds number but friction factor decreases with increasing values of it. The value of $e^+_{opt} = 24$, for one side roughened solar air heater[19], [22], and $e^+_{opt} = 23$, for three sides roughened solar air heaters, presently, differ marginally, which might be due to the two additional roughened sides of the present solar air heater duct. Three sides roughened and glass covered solar air heater has been found to have more value of the heat transfer coefficient than that of one side glass covered roughened solar air heater[23], [24]. The value of e^+_{opt}, is mainly

Ashwini Kumar, B. N. Prasad, and K. D. P. Singh, "Thermal and thermo hydraulic performance of three sides artificially roughened solar air heaters," *International Research Journal of Advanced Engineering and Science*, Volume 2, Issue 2, pp. 215-231, 2017.

affected by the values of p/e, e/D and Re. Therefore, optimal thermo hydraulic performance curves for such solar air heaters will be helpfull while designing such solar air heaters to yield in the optimal thermo hydraulic performance for the varying values of mass flow rate and either of the parameter p/e or e/D.

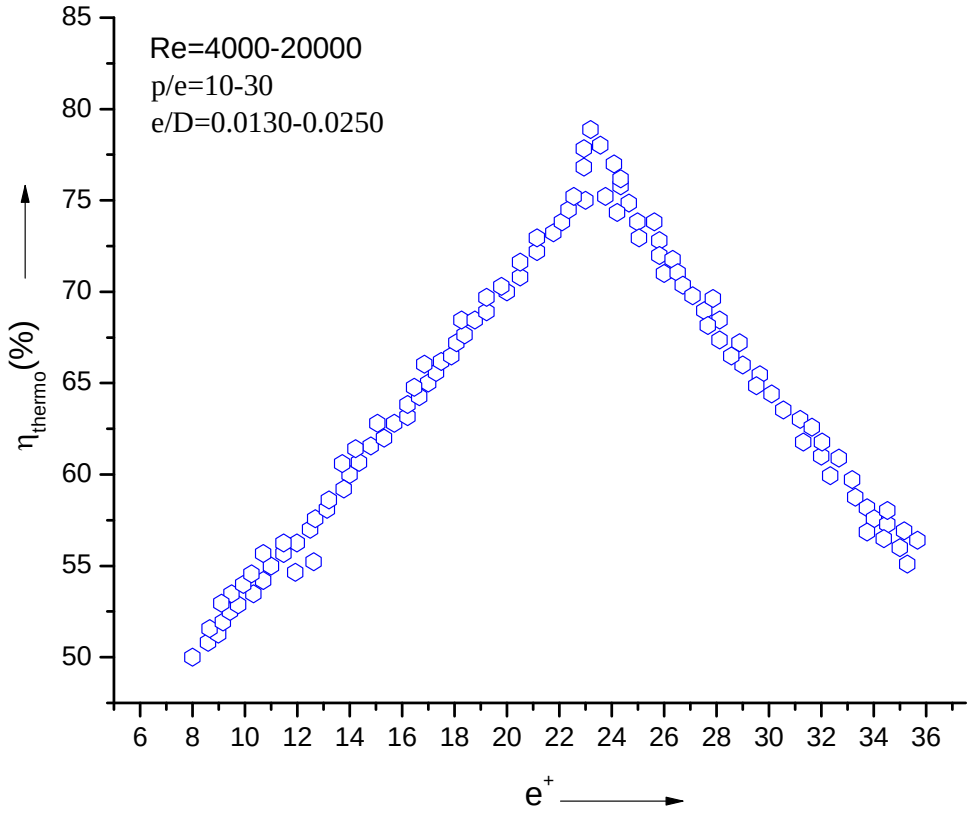

Fig. 22. Optimal thermo hydraulic performance curve.

V. CONCLUSIONS

On the basis of the results and discussions of the present investigation the following conclusions have been drawn:-

1. The values of Stanton number and friction factor in three sides roughened and glass covered solar air heater enhances in the range of 36% to 65% and 28% to 38% respectively over those of three sides glass covered smooth ones.
2. The values of collector heat removal factor, F_R, and collector efficiency factor, F', in such collectors have been found to increase in the range of 51% to 60% and 41% to 49% respectively over those of three sides glass covered smooth ones.
3. Such solar air heaters are thermally 53-57% more efficient than those of three sides glass covered smooth solar air heaters.
4. Roughness Reynolds number, $e^+ = e/D\sqrt{\frac{\bar{f}_r}{2}}Re$, which depends on the roughness geometry and flow parameters, has been optimized to achieve the optimal thermo hydraulic performance in such solar air heaters.
5. The optimal thermo hydraulic performance achieved at $e^+ = 23$, in such solar air heaters, verified the analysis of the authors [25].
6. The value of optimal thermo hydraulic performance corresponding to $e^+_{opt} = 23$ has been found to be about 78.8%.

REFERENCES

[1] B. N. Prasad, J. S. Saini, "Effect of artificial roughness on heat transfer and friction factor in a solar air heater," *Sol. Energy*, vol. 41, pp. 555-560, 1988.
[2] B. N. Prasad, "Thermal performance of artificially roughened solar air heaters," *Sol. Energy*, vol. 91, pp. 59-67, 2013.
[3] V. S. Hans, R. P. Saini, and J. S. Saini, "Heat transfer and friction factor correlations for a solar air heater duct roughened artificially with multiple V-ribs," Sol. Energy, vol. 84, pp. 898-911, 2010.
[4] A. M. Lanjewra, J. L. Bhagoria, and R. M.Sarviya, "Experimental study of augmented heat transfer and friction factor in solar air heater with different orientation of W-Rib roughness," *J. Exp. Therm. Fluid Sci*., vol. 35, pp. 986-995, 2011.

[5] Varun, R. P. Saini, and S. K. Singal, "A review on roughness geometry used in solar air heaters," *Sol. Energy*, vol. 81, pp. 1340-1350, 2007.
[6] U. Shakya, R. P. Saini, and M. K.Singhal, "A review on artificial roughness geometry for enhancement of heat transfer and friction characteristics on roughened duct of solar air heater," *Int. J. Emerg. Technol. Adv. Engg*., vol. 3, pp. 279-287, 2013.
[7] A. S. Yadav and J. L. Bhagoria, "A CFD (computational fluid dynamics) based heat transfer and fluid flow analysis of a solar air heater provided with circular trasverse wire rib roughness on the absorber plate," *Energy*, pp. 1-16, 2013.
[8] S. K. Saini and R. P. Saini, "Development of correlations for Nusselt number and friction factor for solar air heater with roughened duct having arc-shaped wire as artificial roughness," *Sol. Energy*, vol. 82, pp. 1118-1130, 2008.
[9] R. P. Saini and J. Verma, "Heat transfer and friction correlations for a duct having dimple shape artificial roughness for solar air heater," *Energy*, vol. 33, pp. 1277-1287, 2008.
[10] S. Chamoli, N. S. Thakur, and J. S. Saini, "A review of turbulence promoters used in solar thermal system," *Int. J. Renew. Sustain. Energy Rev*., vol. 16, pp. 3154-3175, 2012.
[11] V. B. Gawande, A. S. Dhoble, and D. B. Zodpe, "Effect of roughness geometries on heat transfer enhancement in solar thermal systems- a review," *Renew. Sustain. Energy Rev*., vol. 32, pp. 347-378, 2014.
[12] B. Bhushan and R. Singh, "Thermal and thermo hydraulic performance of roughened solar air heater having protrude absorber plate," *Sol. Energy*, vol. 86, pp. 3388-3396, 2012.
[13] F. Chabane, N. Moummi, and S. Benramache, "Experimental study of heat transfer and thermal performance with longitudinal fins of solar air heater," *J. Adv. Res*., vol. 5, pp. 183-192, 2014.
[14] S. Saurav and M. M. Sahu "Heat transfer and thermal efficiency of solar air heater having artificial roughness: A review," *Int. J. Renew. Energy Res*., vol. 3, pp. 498-508, 2013.
[15] Varun, R. P. Saini, and S. K. Singal, "Investigation on thermal performance of solar air heaters having roughness element as a combination of inclined and trasverse ribs on the absorber plate," *Renew. Energy*, vol. 33, pp. 1398-1405, 2008.
[16] N. Sheriff and P. Gumley, "Heat transfer and friction properties of surfaces with discrete roughness," *Int. J. Heat Mass Trans*., vol. 9, pp. 1297-1320, 1966.
[17] M. J. Lewis, "Optimizing the thermo hydraulic performance of rough surfaces," *Int. J. Heat Mass Trans*., vol. 18, pp. 1243-1248, 1975.
[18] R. L. Webb and E. R. G. Eckert, "Application of rough surfaces to heat exchanger design," *Int. J. Heat Mass Trans*., vol. 15, pp. 1647-1658, 1977.
[19] B. N. Prasad and J. S. Saini, "Optimal thermo-hydraulic performance of artificially roughened solar air heaters," *Sol. Energy*, vol. 47, pp. 91-96, 1991.
[20] S. V. Karmare and A. N. Tikekar, "Experimental investigation of optimum thermo hydraulic performance of solar air heaters with metal rib grits roughness," *Sol. Energy*, vol. 83, pp. 6-13, 2008.
[21] A. Priyam and P. Chand, "Thermal and thermo hydraulic performance of wavy finned absorber solar air heater," *Sol. Energy*, vol. 130, pp. 250-259, 2016.
[22] S. K. Verma and B. N. Prasad, "Investigation for the optimal thermo hydraulic performance of artificially roughened solar air heaters," *Renew. Energy*, vol. 20, pp. 19-36, 2000.
[23] B. N. Prasad, A. K. Behura, and L. Prasad, "Fluid flow and heat transfer analysis for heat transfer enhancement in three sided artificially roughened solar air heater," *Sol. Energy*, vol. 105, pp. 27-35, 2014.
[24] A. K. Behura, B. N. Prasad, and L. Prasad, "Heat transfer, friction factor and thermal performance of three sides artificially roughened solar air heaters," *Sol. Energy*, vol. 130, pp. 46-59, 2016.
[25] B. N. Prasad, A. Kumar, and K. D. P. Singh, "Optimization of thermo hydraulic performance in three sides artificially roughened solar air heaters," *Sol. Energy*, vol. 111, pp. 313-319, 2015.
[26] J. A. Duffie and W. A. Beckman., *Solar Energy Thermal Processes*, Willey Inter-science, New York, 1980.
[27] A. Kumar, B. N. Prasad, and K. D. P. Singh, "Performance characteristics of three sides glass covered smooth solar air heaters," *Transylvanian Review*, vol. 24, issue 11, pp. 3247-3256, 2016.
[28] A. Kumar, K. D. P. Singh, and B. N. Prasad, "Enhancement of collector performance parameters in three sides artificially roughened solar air heater," O P Jindal University, *Conference Proceedings*, 2016.
[29] A. Kumar and M. Alam, "A review on comparative study of thermal performance of artificially roughened solar air heaters," *Int. Research J of Advanced Engineering and Science*, vol. 1, issue 2, pp. 4-12, 2016.
[30] A. Kumar "Thermal performance characteristics of three sides artificially roughened solar air heaters with and without booster mirrors," *Int. Research J of Advanced Engineering and Science*, vol. 1, issue 4, pp. 161-167, 2016.
[31] A. Kumar, "Plate temperature and heat transfer characteristics of three sides roughened and boosted solar air heaters," *Int. Research J of Advanced Engineering and Science*, vol. 1, issue 4, pp. 168-172, 2016.
[32] T. Choudhary and A. Kumar, "Vibration analysis of stiff plate with cutout," *International Journal of Technical Research and Applications*, vol. 3, issue 1, pp. 135-140, 2015.